

# Osteoclast Deficiency Contributes to Temporomandibular Joint Ankylosed Bone Mass Formation

Journal of Dental Research  
2015, Vol. 94(10) 1392–1400  
© International & American Associations  
for Dental Research 2015  
Reprints and permissions:  
sagepub.com/journalsPermissions.nav  
DOI: 10.1177/0022034515599149  
jdr.sagepub.com

L.H. He<sup>1</sup>, E. Xiao<sup>1</sup>, D.H. Duan<sup>2</sup>, Y.H. Gan<sup>3</sup>, and Y. Zhang<sup>1</sup>

## Abstract

Ankylosed bone mass in temporomandibular joint ankylosis (TMJA) is an important factor affecting mouth-opening limitation. However, the mechanism underlying the occurrence of ankylosed bone mass remains unknown. Research has shown that osteoblasts and osteoclasts maintain balance in bone remodeling. Thus, we hypothesized that aberrant osteoclastogenesis and osteogenesis may be involved in the occurrence of ankylosed bone mass in TMJA. In this study, we characterized the osteogenesis of bone marrow stem cells and the osteoclastogenesis of myelomonocyte in clinical specimens of TMJA and normal controls. Results showed that, compared with control bone marrow stem cells, TMJA bone marrow stem cells had lower proliferative and osteogenic capacities. The number of osteoclasts in the ankylosed bone mass group dramatically decreased, and myelomonocyte osteoclastogenic potential was impaired. The RANKL/OPG ratio of the ankylosed bone mass group was lower than that of the control group. Thus, our study suggests that osteoclast deficiency may be an important factor affecting bone mass ankylosis.

**Keywords:** osteoclastogenesis, osteogenesis, bone remodeling, bone marrow stem cells, bone marrow myelomonocytes, pathogenesis

## Introduction

Temporomandibular joint ankylosis (TMJA) leads to chronic, persistent, and progressive mouth-opening inability because the condyle is fused with the glenoid fossa (Maki and Al-Assaf 2008). High-radiodensity ankylosed bone mass is the main feature of TMJA and results in decreased mouth-opening ability (Yan et al. 2011). Although several theories have been proposed to explain the formation of ankylosed bone mass (Norman 1978; Sawhney 1986; Liu et al. 2012; Yan et al. 2012), the underlying physiopathologic mechanisms remain unclear.

Bone formation and bone resorption are essential processes during bone healing, and they maintain the balance of bone remodeling by coupling osteoblasts with osteoclasts. However, when the coupling is not satisfactorily performed, bone diseases occur, such as osteoporosis and osteopetrosis (Gruber et al. 1986; Sobacchi et al. 2007; Sims and Ng 2014). The radiology and histology of ankylosed bone mass make TMJA similar to bone fracture–healing processes (Yan et al. 2013). Our previous studies showed that the mesenchymal stem cells in the radiolucent zone had decreased osteogenic potential and that the bone formation–related genes were downregulated in temporomandibular joint ankylosed callus (Xiao et al. 2013; Yan et al. 2014). Bone marrow ankylosis could also be an important source of osteoblasts and osteoclasts. In the present study, we hypothesized that aberrant osteoclastogenesis and osteogenesis in TMJA bone marrow may be involved in the formation of ankylosed bone mass.

In this study, we evaluated the bone density and osteoclasts of clinical specimens of TMJA, and we characterized the

osteogenesis of bone marrow stem cells (BMSCs) and osteoclastogenesis of bone marrow myelomonocytes (BMMs) derived from the TMJA bone mass.

## Materials and Methods

### Patients

TMJA patients and control subjects were recruited from the Department of Oral and Maxillofacial Surgery, Peking University Hospital of Stomatology. This work was approved

<sup>1</sup>Department of Oral and Maxillofacial Surgery, Peking University School and Hospital of Stomatology, Haidian District, Beijing, China

<sup>2</sup>Department of General Dentistry, Peking University School and Hospital of Stomatology, Haidian District, Beijing, China

<sup>3</sup>Central Laboratory and Center for TMD and Orofacial Pain, Peking University School and Hospital of Stomatology, Haidian District, Beijing, China

A supplemental appendix to this article is published electronically only at <http://jdr.sagepub.com/supplemental>.

### Corresponding Authors:

Y.H. Gan, Central Laboratory and Center for TMD and Orofacial Pain, Peking University School and Hospital of Stomatology, 22 Zhongguancun Nandajie, Haidian District, Beijing 100081, PR China.

Email: [kqyehuagan@bjmu.edu.cn](mailto:kqyehuagan@bjmu.edu.cn)

Y. Zhang, Department of Oral and Maxillofacial Surgery, Peking University School and Hospital of Stomatology, 22 Zhongguancun Nandajie, Haidian District, Beijing 100081, PR China.

Email: [zhangyi2000@263.net](mailto:zhangyi2000@263.net)

by the Ethics Committee of Peking University (IRB00001 05211002), and all participants gave informed consent. Patient information is listed in Appendix Tables 1 and 2.

### **Bone Parameter Analysis of Normal Condyle and TMJA Bone Mass**

The bone parameters were analyzed as previously described (O'Neill et al. 2012). Computed tomography (CT) data (helix with 1.25-mm slice thickness; Bright Speed 16, GE Healthcare, Buckinghamshire, UK) were transferred to the Inveon Research Workplace (SIEMENS, Munich, Germany). The region of interest was depicted, and the CT values were calculated. The procedures are described in the Appendix.

### **Tartrate-resistant Acid Phosphatase Staining**

Tartrate-resistant acid phosphatase (TRAP) staining was performed as previously described (Li et al. 2014; Yang et al. 2014) on the clinical specimens of resected ankylosed bone masses from 14 patients with posttraumatic TMJA, which were classified according to the Sawhney classification. The control condyle was obtained from a patient with mandibular ramus tumor that did not involve the condyle. For each sample, 3 sections were randomly selected from the anterior, middle, and posterior parts of the bone mass and then stained with TRAP (Sigma-Aldrich, St. Louis, MO, USA) according to the manufacturer's instructions. The detailed procedures are described in the Appendix. The osteoclasts were counted within the bone marrow from 3 random views per section and averaged by the total length of the circumference of the bone marrow via a BIOQUANT OSTEO Bone Biology Research System (BIOQUANT Image Analysis Corporation, Nashville, TN, USA). The osteoclast number per bone marrow (i.e., per circumference of bone marrow in millimeters) was presented for each group.

### **Isolation of BMSCs and BMMs from Bone Tissues**

BMSCs and BMMs were isolated from type II or III ankylosed bone masses and from the mandibular bone marrow of the control subjects. The mandibular bone marrow was acquired when the control subjects underwent tooth extraction or orthopedic surgery. No patient or control subject had an infectious or systemic disease. The BMSCs were isolated from bone tissues as previously described (Xiao et al. 2013). The BMSCs and the BMMs were collected and cultured at 37 °C in a humidified atmosphere of 5% CO<sub>2</sub> and 95% air. The detailed procedures are available in the Appendix.

### **Colony-forming Unit Assay**

Colony-forming unit assays were performed as previously described (Cheng et al. 2009). The procedures are described in the Appendix.

### **Flow Cytometry Analysis**

Flow cytometry analysis was conducted as previously described (Xiao et al. 2013). The detailed information and procedures are available in the Appendix.

### **Multidifferentiation Assays**

The third-passage cells were cultured in osteogenic, adipogenic, and chondrogenic media in vitro. The details are described in the Appendix.

### **Cell Proliferation Assays**

The cell proliferation assays were conducted and are described in the Appendix.

### **Osteoclast Differentiation In Vitro**

The BMMs were collected and induced for osteoclast precursor cells, which were equally seeded and further cultured in the osteoclast differentiation medium to induce the osteoclasts. The cells were then stained with TRAP, and the 3-nucleated TRAP<sup>+</sup> cells identified as the osteoclasts were counted from 5 wells of a 96-well plate for each sample. The data were presented as cell number per well. The procedures are described in the Appendix.

### **Alkaline Phosphatase Staining Assay**

Alkaline phosphatase (ALP) staining was conducted according to the manufacturer's instructions. Detailed information is available in the Appendix.

### **RNA Isolation and Real-time Polymerase Chain Reaction**

RNA isolation and real-time polymerase chain reaction were conducted as previously described and are detailed in the Appendix. The primers used are listed in the Table.

### **Western Blot Assay**

Western blot assay was conducted as previously described (see Appendix). Primary antibodies for Runx2 (Biogot Technology Co. Ltd., Nanjing, China) and β-actin (Santa Cruz Biotechnology, Inc., Santa Cruz, CA, USA) were used to detect the target proteins.

### **Enzyme-linked Immunosorbent Assay**

Enzyme-linked immunosorbent assay (ELISA; BD Biosciences, San Jose, CA, USA) was conducted according to the manufacturer's instructions. The RANKL and OPG relative concentrations were determined, and the RANKL/OPG ratio was calculated, as described in the Appendix.

**Table.** Primers Used in Real-time Polymerase Chain Reaction Gene Expression Analysis.

Gene	Primer Sequences (5'-3')
$\beta$ -actin	
Forward	CATGTACGTTGCTATCCAGGC
Reverse	CTCCTTAATGTCACGCACGAT
Runx2	
Forward	TGGTTACTGTCATGGCGGGTA
Reverse	TCTCAGATCGTTGAACCTTGCTA
ALP	
Forward	GAACGTGGTCACCTCCATCCT
Reverse	TCTCGTGGTCACAATGC
OPN	
Forward	CTCCATTGACTCGAACGACTC
Reverse	CAGGCTGCGAAACTTCTTAGAT
RANKL	
Forward	ACATATCGTTGGATCACAGCACAT
Reverse	CAAAAGGCTGAGCTTCAAGCTT
OPG	
Forward	GGAACCCAGAGCGAAATACA
Reverse	CCTGAAGAATGCCTCTCACA

### Statistical Analysis

Data are presented as mean  $\pm$  SD and were analyzed with SPSS 18.0 software (SPSS Inc., Chicago, IL, USA). The values about osteogenesis of BMSCs, osteoclastogenesis of BMMs, and the ratio of RANKL/OPG were tested by independent Student's *t* tests. The values about bone parameters compared among 5 groups and the values about the relative osteoclast number in vivo were tested by Student-Newman-Keuls test. The values about bone parameters compared between control condyle and TMJA bone mass were tested by paired-sample *t* test. The Kolmogorov-Smirnov test was chosen to test the normal distribution.  $P < 0.05$  was considered statistically significant.

## Results

### Ankylosed Bone Mass Showed Higher Bone Mineral Density Than Normal Condyle

The ankylosed bone mass of TMJA always had a higher bone mineral density than the normal condyle, as confirmed by the CT images (Fig. 1A). The ankylosed bone mass was obvious in types II to IV ankylosis but not in type I ankylosis. The bone volume/total volume and the trabecular bone thickness of the ankylosed bone mass progressively increased with ankylosis severity as compared with normal condyle (Fig. 1B–G;  $P < 0.05$ ). Yet, the trabecular space and the bone surface/bone volume of ankylosed bone mass progressively decreased with ankylosis severity as compared with normal condyle (Fig. 1H–I;  $P < 0.05$ ).

### BMSCs Derived from Ankylosis Bone Mass Showed Lower Proliferative Capacity Than BMSCs Derived from Mandibular Bone

We first examined the proliferative capacity of BMSCs in the ankylosed bone mass. As shown in Figure 2C, the colony-forming

efficiency of BMSCs isolated from the ankylosed bone mass was lower than that of BMSCs from the mandibular bone marrow ( $69.67\% \pm 12.5\%$ ;  $P < 0.05$ ; Fig. 2D), and the proliferation rate of BMSCs isolated from the ankylosed bone mass was also lower than that of BMSCs from the mandibular bone marrow on days 4, 6, 8, 10, and 12 (Fig. 2E). BMSCs isolated from the ankylosed bone mass and mandibular bone marrow were confirmed to be multipotent cells, which can form mineralized matrix and lipid or exhibit chondrogenic capability (Fig. 2F). Moreover, both cells expressed surface markers of BMSCs, including CD73, CD90, and CD105, but were negative for CD34 and CD45 (Fig. 2G).

### BMSCs Derived from Ankylosed Bone Mass Exhibited Decreased Osteogenic Potential Than That Derived from the Mandibular Bone

The alizarin red staining results show that the calcium deposition of BMSCs from the type II (A2, A4) or type III (A1, A3, A5) ankylosed bone mass was less than that from the mandibular bone marrow on day 21 (Fig. 3A). On day 7, ALP staining results revealed that BMSCs from type II or type III ankylosed bone mass were also less than that from the mandibular bone marrow (Fig. 3B). Correspondingly, the mRNA expressions of Runx2, ALP, OPN, and Runx2 proteins in BMSCs from the type II or type III ankylosed bone mass were lower than those from the mandibular bone during osteoblastic differentiation (Fig. 3C, D).

### Decreased Osteoclasts and Impairment of Osteoclastogenic Potential of BMMs from Ankylosed Bone Mass

Explaining ankylosed bone mass based only on BMSCs is difficult and incomprehensive. Moreover, osteoclasts are essential cells that contribute to bone dynamic balance. Thus, we then analyzed the osteoclastogenesis of the ankylosed bone mass. In type I ankylosis, the multinucleated osteoclasts were abundant (Fig. 4A, b1–b3). In type II ankylosis, the multinucleated osteoclasts were hardly visible (Fig. 4A, c1–c3). In types III and IV ankylosis, the multinucleated osteoclasts were deficient in number (Fig. 4A, d1–d3 and e1–e3). To further evaluate the osteoclastogenic potential of the BMMs from temporomandibular joint ankylosis ankylosed bone marrow, osteoclast differentiation assays and in vitro TRAP staining were conducted. After induction of BMMs from the ankylosed bone masses of 4 patients, the multinuclear osteoclasts were much less than that of BMMs from the mandible bone marrow of 4 control subjects (Fig. 4B). Correspondingly, the quantitative results of the osteoclasts in the clinical samples showed that the osteoclasts per bone marrow (i.e., per circumference of bone marrow in millimeters) was also abundant in type I ankylosis, dramatically decreased in type II ankylosis, and deficient in types III and IV ankylosis (Fig. 4C). The quantitative results of osteoclast in vitro assay showed that the number of TRAP<sup>+</sup> multinucleated osteoclasts per well formed from mandibular

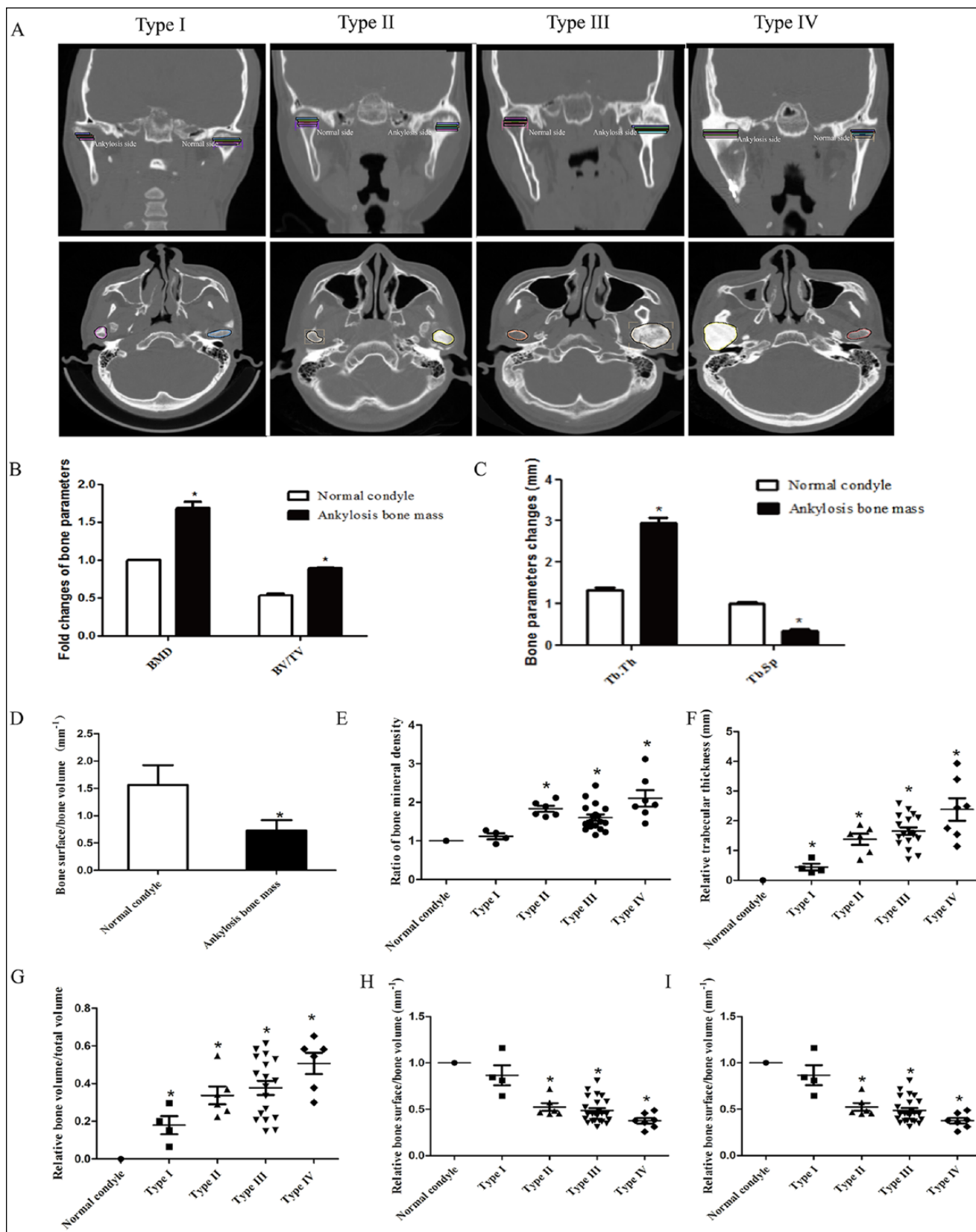


**Figure 1.** Quantitative analysis of ankylotic bone mass and normal condyle. (A) Representative computed tomography images of 4 types of temporomandibular joint ankylosis. The region of interest is shown in the coronal and axial planes, and 5 sequential axial images were analyzed. (B–I) Quantitative results of ankylotic bone mass. BMD, bone mineral density; BV/TV, bone volume/total volume; Tb.Th, trabecula bone thickness; Tb.Sp, trabecula space. \**P* < 0.05 versus normal condyle. Quantification was based on the samples of 35 healthy patients and 35 ankylosis patients, including 4, 6, 18, and 7 patients with types I–IV ankylosis, respectively. Note: no statistically significant difference was observed in the BMD of type I ankylosis and the control condyle in (E).

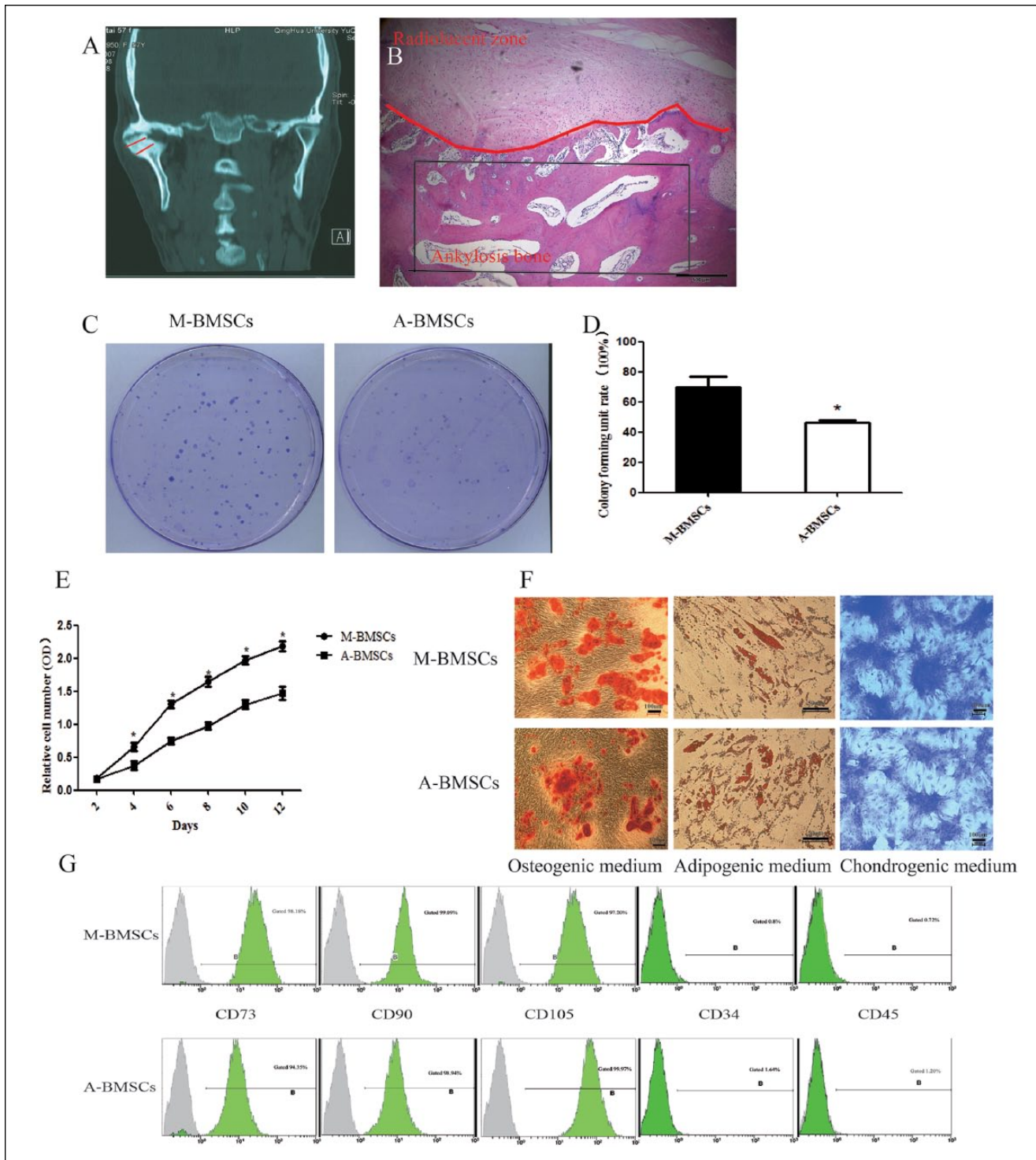


**Figure 2.** Characterization of bone marrow stem cells (BMSCs). (A) Computed tomography shows where the bone mass was excised. (B) Micro-photograph of the representative section of bone mass. The red line shows the boundary between the bone marrow and the fibrocartilage tissue. (C, D) Colony-forming capacity of BMSCs. \* $P < 0.05$  versus M-BMSCs. (E) Proliferative capacity of BMSCs. \* $P < 0.05$  versus M-BMSCs. (F) Multilineage differentiation of BMSCs. (G) Identification of BMSCs with different marks. M-BMSCs, BMSCs from the mandibular bone marrow of 5 control subjects; A-BMSCs, BMSCs from 5 patients with type II or III ankylosis.

BMMs was much higher than that from ankylosed BMMs (type II to III; Fig. 4D). To further explore the mechanism of osteoclast deficiency in the ankylosed bone mass, the total mRNA and protein expression of bone mass were determined

by real-time polymerase chain reaction and ELISA assays. The mRNA ratio of RANKL/OPG of the ankylosed bone mass was also lower than that of the mandibular bone (Fig. 4E). Moreover, the ELISA result also showed that the ratio of

RANKL/OPG decreased in the temporomandibular joint ankylosis ankylosed bone mass (Fig. 4F).

## Discussion

In this study, we quantitatively compared the bone density of ankylosed bone mass of TMJA with normal condyle and found that BMSCs and BMMs derived from the ankylosed bone mass showed lower osteogenic potential and impaired osteoclastogenesis ability, respectively.

The ankylosed bone mass of TMJA was less likely due to excessive bone formation. The bone marrow is believed to have important functions during fracture healing by providing niches for hematopoietic and mesenchymal stem cells (Taguchi et al. 2005; Ueno et al. 2011). Accordingly, ankylosed bone mass of TMJA is believed to be related to the high osteogenic potential of BMSCs. However, the osteogenic potential of BMSCs from the ankylosed bone mass unexpectedly decreased compared with that of BMSCs from normal mandibular bone marrow. The decreased osteogenic potential of BMSCs meant slow bone formation. Since the BMSCs from the ankylosed bone mass showed lower osteogenic potential than the normal control BMSCs, the formation of the ankylosed bone mass could not be fully explained by the aberrant BMSCs. Bone remodeling is maintained by bone formation and bone resorption (Tanaka et al. 2005). Therefore, ankylosed bone mass of TMJA could also be caused by impaired bone resorption process, which is also the case for particular osteopetrosis diseases or bone nonunion (Helfrich 2003; Gerstenfeld et al. 2009). Nevertheless, the decreased osteogenic potential of BMSCs in the ankylosed bone mass meant that the formation of ankylosed bone mass would take a longer time, and this phenomenon perfectly explains the long-term history of TMJA.

Decreased osteoclastogenesis is an important factor that contributed to the occurrence of ankylosed bone mass of TMJA. Osteoclasts are indispensable and have critical functions during bone fracture healing (Tanaka et al. 2005; Matsuo and Irie 2008). When osteoclast formation is impaired and the resorptive capacity is deficient, the bone resorption process will be impeded and lead to progressively increased bone density in patients afflicted with particular osteopetrosis diseases or bone nonunion (Helfrich 2003; Gerstenfeld et al. 2009). We

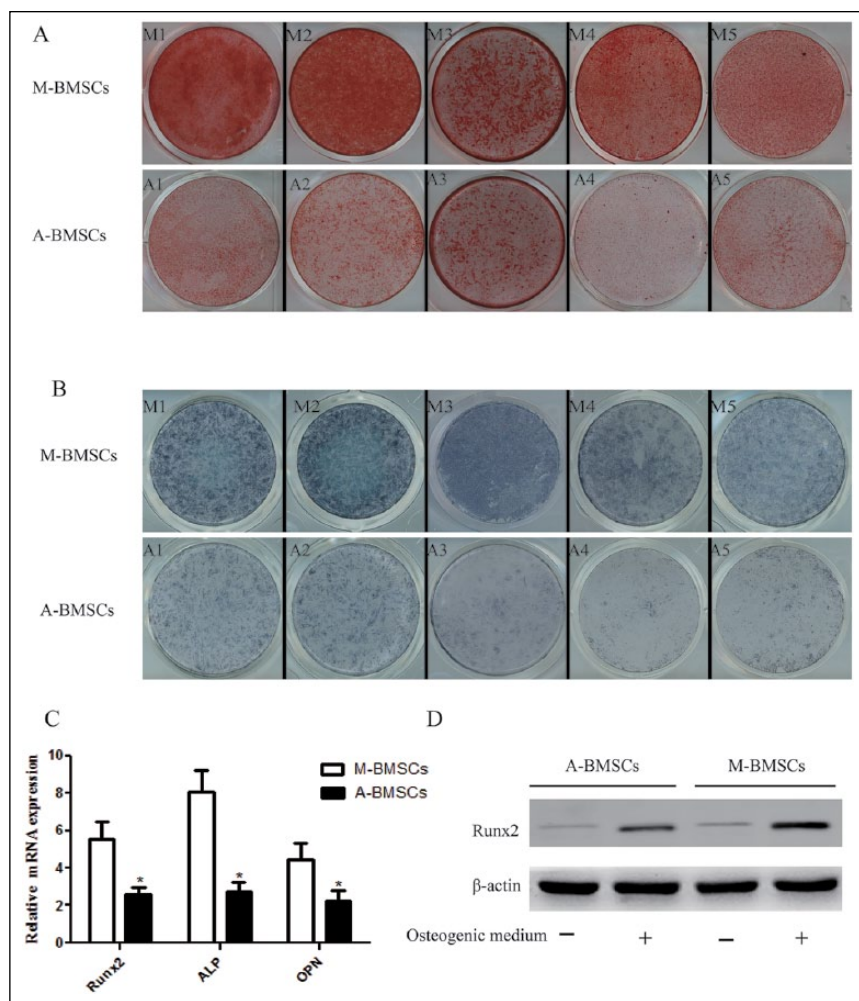


**Figure 3.** Osteogenic potential of bone marrow stem cells (BMSCs). **(A)** Alizarin red staining of calcium deposition of BMSCs from 5 patients and 5 control subjects. **(B)** Alkaline phosphatase (ALP) staining for ALP activity of BMSCs from 5 patients with type II or III ankylosis and 5 control subjects. **(C)** mRNA expression of genes in BMSCs was quantitatively evaluated via real-time PCR. \* $P < 0.05$  versus M-BMSCs. **(D)** Western blot analysis of Runx2 expression in BMSCs after osteogenic induction. M1-M5, BMSCs from the mandibular bone marrow of 5 control subjects; A1-A5, BMSCs from ankylosed bone masses of 5 patients with type II (A2 and A4) or type III (A1, A3, and A5) ankylosis; M-BMSCs, BMSCs from the mandibular bone marrow of 5 control subjects; A-BMSCs, BMSCs from ankylosed bone masses of 5 patients with type II or III ankylosis.

observed that osteoclasts were abundant in type I ankylosis, and abundant osteoclasts can efficiently and rapidly resorb redundant bone. Thus, patients with type I ankylosis did not show obvious ankylosed bone mass. However, in ankylosis types II to IV, the number of osteoclasts per bone marrow (i.e., circumference of bone marrow in millimeters) dramatically decreased. Furthermore, the osteoclastogenic potential of the BMMs in ankylosed bone mass was also impaired in vitro compared with that of BMMs from the mandible bone marrow of control subjects. This in vitro result could explain, to an extent, the decrease in osteoclasts in the ankylosed bone mass. Studies have noted that a deficiency of osteoclasts causes severe osteopetrosis diseases (Li et al. 2000; Sobacchi et al. 2007). Therefore, our results suggest that ankylosed bone mass of TMJA would be mainly due to osteoclast deficiency.

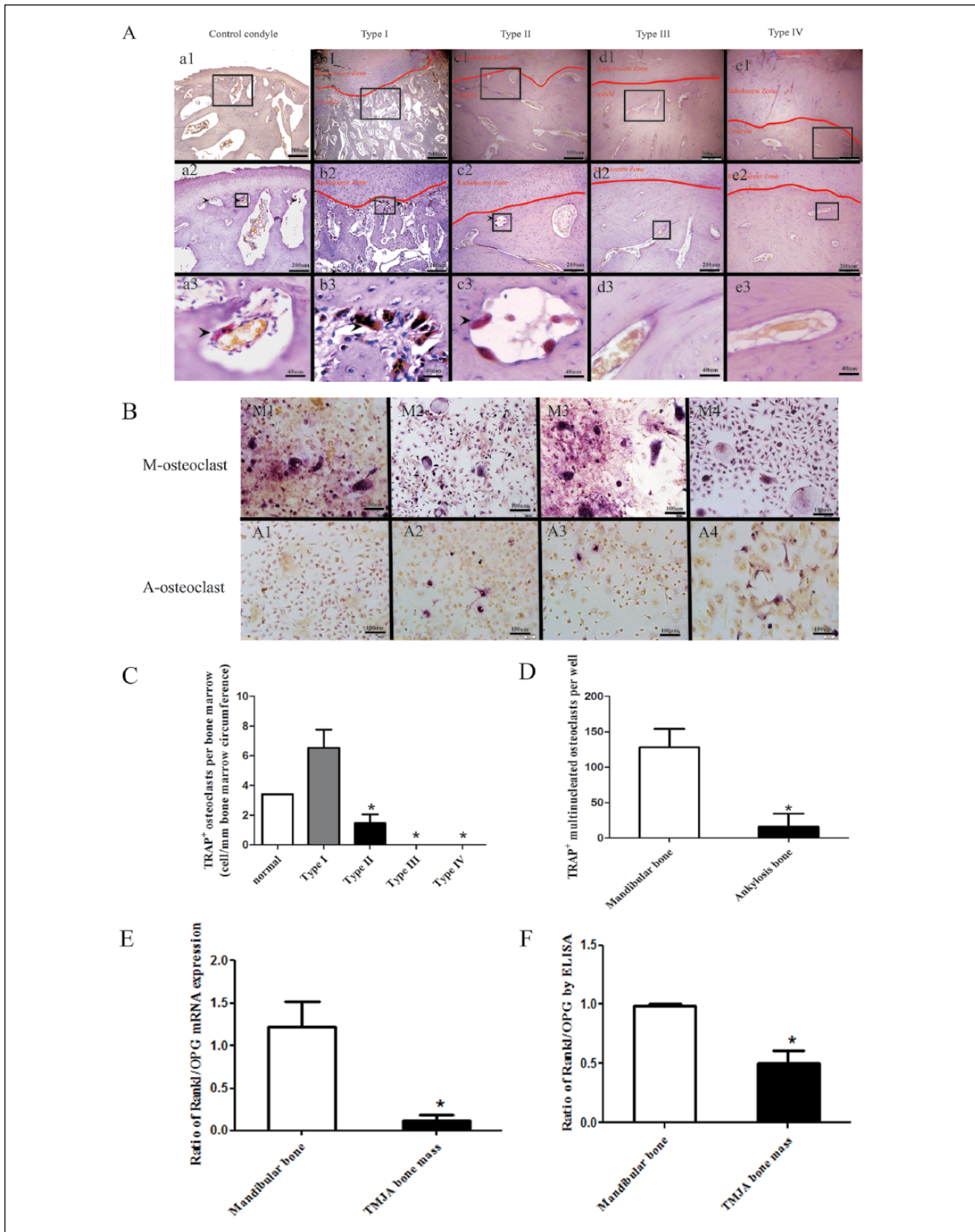


**Figure 4.** Decrease in osteoclasts and osteoclastogenesis potential in ankylotic bone mass. **(A)** TRAP staining of osteoclasts in the ankylotic bone mass and control mandibular bone. The larger black boxes in a1-e1 indicate from where a2-e2 were magnified, and the smaller black boxes in a2-e2 indicate from where a3-e3 were magnified. The arrowheads indicate TRAP staining-positive osteoclasts. **(B)** Osteoclastogenic potential of bone marrow myelomonocytes (BMMs). M1-M4, BMMs from the mandibular bone marrow of 4 control subjects; A1-A4, BMMs from the ankylotic bone masses of 4 patients with type II or III ankylosis. **(C, D)** Quantitative analysis of osteoclasts in **(A)** (\**P* < 0.05 versus normal condyle) and **(B)** (\**P* < 0.05 versus mandibular bone). **(E)** Ratio of RANKL/OPG mRNA expression was evaluated by real-time PCR in 4 ankylotic bone masses and 3 mandibular bones. **(F)** Ratio of RANKL/OPG protein expression was evaluated by ELISA.

A low RANKL/OPG ratio was related to osteoclast deficiency in the TMJA bone mass. The RANKL-RANK-OPG system is the most important signaling pathway involved in osteoclastogenesis during bone healing (Pivonka et al. 2010). Our results showed that the ratio of RANKL/OPG decreased in the ankylosed bone mass compared with that of the control group. This result could help explain why the osteoclasts and osteogenic potential of BMMs in the ankylosed bone mass decreased. However, the reason for the decrease in the ratio of RANKL/OPG in the ankylosed bone mass remains unclear. The mechanism may be related to the inhibition of osteoclastogenesis by the BMSCs and osteocytes by decreasing the RANKL/OPG ratio at shear stress conditions (Cackowski et al. 2010; Cui et al. 2012) when complex mechanical stresses exist in a TMJA microenvironment.

High bone mineral density is the main characteristic of TMJA bone mass. Previous studies identified that quantitative bone parameter analysis is an effective method to assess the remodeling process of a fractured callus (Nyman et al. 2009). Although several studies noted that TMJA bone mass is featured with high bone mineral density, based on CT images (Yan et al. 2012; Li et al. 2014), these studies lacked quantitative results. Our study first quantitatively confirmed that ankylosed bone mass had higher bone mineral density, trabecular bone thickness, and bone volume/total volume than did normal control subjects, and these characteristics were also reflected in the lower bone surface/bone volume. A previous study indicated that the bone surface/bone volume decreased but the trabecular bone thickness and bone volume/total volume increased after alendronate treatment in osteoporotic women (Recker et al. 2005). These results are consistent with those obtained for the osteopetrotic callus (Lee et al. 2006) and suggest the imbalance between bone formation and bone resorption in TMJA.

In conclusion, our results show that the osteogenic potential of BMSCs and the number of osteoclasts and rate of osteoclastogenesis of BMMs decreased in the ankylosed bone mass. The occurrence of ankylosed bone mass of TMJA could be mainly due to the decreased number of osteoclasts in ankylosed bone mass.

### Author Contributions

L.H. He, contributed to conception and design, drafted the manuscript; E. Xiao, contributed to data analysis, critically revised the manuscript; D.H. Duan, contributed to data acquisition, critically revised the manuscript; Y.H. Gan, contributed to data analysis and interpretation, critically revised the manuscript; Y. Zhang, contributed to conception and design, critically revised the manuscript. All authors gave final approval and agree to be accountable for all aspects of the work.

### Acknowledgments

This work was supported by a grant from the National Natural Science Foundation of China (81170936) and Beijing Natural Science Foundation (7152155). The authors declare no potential conflicts of interest with respect to the authorship and/or publication of this article.

### References

- Cackowski FC, Anderson JL, Patrene KD, Choksi RJ, Shapiro SD, Windle JJ, Blair HC, Roodman GD. 2010. Osteoclasts are important for bone angiogenesis. *Blood*. 115(1):140–149.
- Cheng MT, Yang HW, Chen TH, Lee OK. 2009. Isolation and characterization of multipotent stem cells from human cruciate ligaments. *Cell Prolif*. 42(4):448–460.
- Cui L, Li XT, Zhang D. 2012. Effect of fluid flow-induced shear stress on osteoclast formation induced by osteocyte. *Zhongguo Yi Xue Ke Xue Yuan Xue Bao*. 34(3):207–211.
- Gerstenfeld LC, Sacks DJ, Pelis M, Mason ZD, Graves DT, Barrero M, Ominsky MS, Kostenuik PJ, Morgan EF, Einhorn TA. 2009. Comparison of effects of the bisphosphonate alendronate versus the RANKL inhibitor denosumab on murine fracture healing. *J Bone Miner Res*. 24(2):196–208.
- Gruber HE, Ivey JL, Thompson ER, Chesnut CR, Baylink DJ. 1986. Osteoblast and osteoclast cell number and cell activity in postmenopausal osteoporosis. *Miner Electrolyte Metab*. 12(4):246–254.
- Helfrich MH. 2003. Osteoclast diseases. *Microsc Res Tech*. 61(6):514–532.
- Lee SH, Rho J, Jeong D, Sul JY, Kim T, Kim N, Kang JS, Miyamoto T, Suda T, Lee SK, et al. 2006. v-ATPase V0 subunit d2-deficient mice exhibit impaired osteoclast fusion and increased bone formation. *Nat Med*. 12(12):1403–1409.
- Li J, Mori S, Kaji Y, Kawanishi J, Akiyama T, Norimatsu H. 2000. Concentration of bisphosphonate (incadronate) in callus area and its effects on fracture healing in rats. *J Bone Miner Res*. 15(10):2042–2051.
- Li JM, An JG, Wang X, Yan YB, Xiao E, He Y, Zhang Y. 2014. Imaging and histologic features of traumatic temporomandibular joint ankylosis. *Oral Surg Oral Med Oral Pathol Oral Radiol*. 118(3):330–337.
- Liu CK, Liu P, Meng FW, Deng BL, Xue Y, Mao TQ, Hu KJ. 2012. The role of the lateral pterygoid muscle in the sagittal fracture of mandibular condyle (SFM) healing process. *Br J Oral Maxillofac Surg*. 50(4):356–360.
- Maki MH, Al-Assaf DA. 2008. Surgical management of temporomandibular joint ankylosis. *J Craniofac Surg*. 19(6):1583–1588.
- Matsuo K, Irie N. 2008. Osteoclast-osteoblast communication. *Arch Biochem Biophys*. 473(2):201–209.
- Norman JE. 1978. Ankylosis of the temporomandibular joint. *Aust Dent J*. 23(1):56–66.
- Nyman JS, Munoz S, Jadhav S, Mansour A, Yoshii T, Mundy GR, Gutierrez GE. 2009. Quantitative measures of femoral fracture repair in rats derived by micro-computed tomography. *J Biomech*. 42(7):891–897.
- O'Neill KR, Stutz CM, Mignemi NA, Burns MC, Murry MR, Nyman JS, Schoenecker JG. 2012. Micro-computed tomography assessment of the progression of fracture healing in mice. *Bone*. 50(6):1357–1367.
- Pivonka P, Zimak J, Smith DW, Gardiner BS, Dunstan CR, Sims NA, Martin TJ, Mundy GR. 2010. Theoretical investigation of the role of the RANK-RANKL-OPG system in bone remodeling. *J Theor Biol*. 262(2):306–316.
- Recker R, Masarachia P, Santora A, Howard T, Chavassieux P, Arlot M, Rodan G, Wehren L, Kimmel D. 2005. Trabecular bone microarchitecture after alendronate treatment of osteoporotic women. *Curr Med Res Opin*. 21(2):185–194.
- Sawhney CP. 1986. Bony ankylosis of the temporomandibular joint: follow-up of 70 patients treated with arthroplasty and acrylic spacer interposition. *Plast Reconstr Surg*. 77(1):29–40.
- Sims NA, Ng KW. 2014. Implications of osteoblast-osteoclast interactions in the management of osteoporosis by antiresorptive agents denosumab and odanacatib. *Curr Osteoporos Rep*. 12(1):98–106.
- Sobacchi C, Frattini A, Guerrini MM, Abinun M, Pangrazio A, Susani L, Bredius R, Mancini G, Cant A, Bishop N, et al. 2007. Osteoclast-poor human osteopetrosis due to mutations in the gene encoding RANKL. *Nat Genet*. 39(8):960–962.
- Taguchi K, Ogawa R, Migita M, Hanawa H, Ito H, Orimo H. 2005. The role of bone marrow-derived cells in bone fracture repair in a green fluorescent protein chimeric mouse model. *Biochem Biophys Res Commun*. 331(1):31–36.
- Tanaka Y, Nakayamada S, Okada Y. 2005. Osteoblasts and osteoclasts in bone remodeling and inflammation. *Curr Drug Targets Inflamm Allergy*. 4(3):325–8.
- Ueno M, Uchida K, Takaso M, Minehara H, Suto K, Takahira N, Steck R, Schuetz MA, Itoman M. 2011. Distribution of bone marrow-derived cells in the fracture callus during plate fixation in a green fluorescent protein-chimeric mouse model. *Exp Anim*. 60(5):455–462.
- Xiao E, Li JM, Yan YB, An JG, Duan DH, Gan YH, Zhang Y. 2013. Decreased osteogenesis in stromal cells from radiolucent zone of human TMJ ankylosis. *J Dent Res*. 92(5):450–455.
- Yan YB, Zhang Y, Sun Z, Li J, Xiao E, An J. 2011. The relationship between mouth opening and computerized tomographic features of posttraumatic



- bony ankylosis of the temporomandibular joint. *Oral Surg Oral Med Oral Pathol Oral Radiol Endod.* 111(3):354–361.
- Yan YB, Duan DH, Zhang Y, Gan YH. 2012. The development of traumatic temporomandibular joint bony ankylosis: a course similar to the hypertrophic nonunion. *Med Hypotheses.* 78(2):273–276.
- Yan YB, Zhang Y, Gan YH, An JG, Li JM, Xiao E. 2013. Surgical induction of TMJ bony ankylosis in growing sheep and the role of injury severity of the glenoid fossa on the development of bony ankylosis. *J Craniomaxillofac Surg.* 41(6):476–486.
- Yan YB, Li JM, Xiao E, An JG, Gan YH, Zhang Y. 2014. A pilot trial on the molecular pathophysiology of traumatic temporomandibular joint bony ankylosis in a sheep model: part II. The differential gene expression among fibrous ankylosis, bony ankylosis and condylar fracture. *J Craniomaxillofac Surg.* 42(2):e23–e28.
- Yang T, Zhang J, Cao Y, Zhang M, Jing L, Jiao K, Yu S, Wang M. 2014. Decreased bone marrow stromal cells activity involves in unilateral anterior crossbite-induced early subchondral bone loss of temporomandibular joints. *Arch Oral Biol.* 59(9):962–969.